

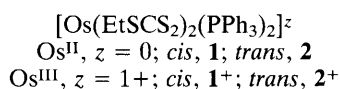
Differentiation of Isomeric Coordination Geometries by Metal Valence: A Structural Study of its Origin in $[\text{Os}(\text{EtSCS}_2)_2(\text{PPh}_3)_2]^z$ ($z = 0$ and $1+$)

Amitava Pramanik, Nilkamal Bag, Debashis Ray, Goutam Kumar Lahiri and Animesh Chakravorty*

Department of Inorganic Chemistry, Indian Association for the Cultivation of Science, Calcutta 700032, India

In the title complexes Os^{II} and Os^{III} display strong preferences for *cis*- and *trans*- S_4P_2 geometries respectively; structural parameters of the *cis*- Os^{II} , *trans*- Os^{II} and *trans*- Os^{III} isomers have revealed that back-bonding and steric crowding within the $\text{Os}(\text{PPh}_3)_2$ fragment are the primary controlling factors.

This work stems from our interest in the recognition and differentiation of geometrically isomeric coordination spheres by different oxidation states of the same metal ion.¹⁻⁴ Owing to the lack of availability of X-ray quality crystals it has not hitherto been possible to probe the origin of this phenomenon directly. We now describe such a study on the Os complexes **1**, **2**, and **2**⁺.



The complexes were synthesised by the reactions in eqns. (1)–(3). Reaction (1) occurs quantitatively in boiling ethanol affording **1** as yellow crystals.† In reaction (2) a MeCN– CH_2Cl_2 solution of **1** is oxidised by aqueous Ce^{IV} ; the resulting bluish green cation **2**⁺ is isolated as its PF_6^- salt. Complex **2** is obtained as a pale-green solid by reduction of **2**⁺ with

$\text{N}_2\text{H}_4 \cdot \text{H}_2\text{O}$ in cold MeCN, reaction (3). The X-ray structures‡ of **1**, **2** and **2**⁺ are shown in Figs. 1 and 2. To the best of our

‡ Crystal data for **1**: $\text{C}_{42}\text{H}_{40}\text{P}_2\text{S}_6\text{Os}$, $M_r = 989.2$, monoclinic, space group $C2/c$, $Z = 4$, $a = 23.292(6)$, $b = 10.850(4)$, $c = 17.353(3)$ Å, $\beta = 113.19(2)^\circ$, $V = 4031(2)$ Å³, $T = 295\text{K}$, $D_c = 1.630$ g cm⁻³, $\mu(\text{Mo-K}\alpha) = 35.74$ cm⁻¹, crystal dimensions $0.18 \times 0.20 \times 0.44$ mm³. For **2**: $\text{C}_{42}\text{H}_{40}\text{P}_2\text{S}_6\text{Os}$, triclinic, space group $P\bar{1}$, $Z = 1$, $a = 9.654(4)$, $b = 10.348(6)$, $c = 12.026(7)$ Å, $\alpha = 65.24(4)$, $\beta = 88.61(4)$, $\gamma = 70.75(4)^\circ$, $V = 1020.8(9)$ Å³, $T = 295\text{K}$, $D_c = 1.609$ g cm⁻³, $\mu(\text{Mo-K}\alpha) = 35.28$ cm⁻¹, crystal dimensions $0.20 \times 0.12 \times 0.44$ mm³. For **2**⁺: $\text{C}_{42}\text{H}_{40}\text{F}_6\text{P}_3\text{S}_6\text{Os}$, $M_r = 1134.2$, triclinic, space group $P\bar{1}$, $Z = 1$, $a = 9.752(4)$, $b = 11.747(3)$, $c = 11.939(4)$ Å, $\alpha = 62.28(2)$, $\beta = 78.99(3)$, $\gamma = 67.94(3)^\circ$, $V = 1121.8(6)$ Å³, $T = 295\text{K}$, $D_c = 1.679$ g cm⁻³, $\mu(\text{Mo-K}\alpha) = 32.74$ cm⁻¹, crystal dimensions $0.36 \times 0.18 \times 0.22$ mm³. Data were collected in the range $2.0 \leq 2\theta \leq 55.0^\circ$ on a Nicolet R3m/V four-circle diffractometer. 4593 and 4583 independent reflections were collected respectively for **1** and **2** by the ω -scan technique of which 2626 and 3955 reflections had $I > 3\sigma(I)$. For **2**⁺, the 2θ -scan technique was used to collect 5189 unique reflections of which 5020 had $I > 3\sigma(I)$. The $I > 3\sigma(I)$ reflections were used for structure solution. An empirical absorption correction was done on the basis of azimuthal scans.⁷ All calculations used the SHELXTL-Plus⁸ program package. All the structures were solved by direct methods and subsequently refined by full-matrix least-squares procedures. Two phenyl rings [C(4)–C(9) and C(16)–C(21)] in **1** are shown in the 'Affixed' condition but were actually disordered. All non-hydrogen atoms (except disordered carbon atoms) were refined with anisotropic thermal parameters. Hydrogen atoms were included (except for those on the disordered carbons) at calculated positions with U -values of 0.08 Å². The structures refined to $R = 5.04$ and $R_w = 6.09\%$ for **1**; $R = 5.83$ and $R_w = 6.92\%$ for **2**; and $R = 3.05$ and $R_w = 4.11\%$ for **2**⁺. The highest difference Fourier peaks were 0.71 , 0.61 and 0.66 e Å⁻³ near the metal atom for **1**, **2** and **2**⁺ respectively. Atomic coordinates, bond distances and angles, and thermal parameters have been deposited at the Cambridge Crystallographic Data Centre. See Notice to Authors, Issue No. 1.

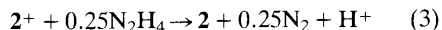
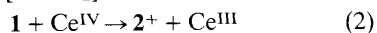
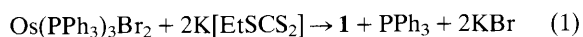
Table 1 Formal potentials and equilibrium constants at 303 K

$E_{\text{cis}}^\circ/\text{V}^a$	$E_{\text{trans}}^\circ/\text{V}^a$	K_{II}^b	K_{cr}^c	K_{III}^d
0.43	0.15	8.33	4.53×10^4	5.40×10^3

^a Cyclic voltammetry at Pt electrode vs. standard calomel electrode in dichloromethane, supporting electrolyte $[\text{NEt}_4][\text{ClO}_4]$, scan rate 50 mV s⁻¹. ^b $K_{\text{II}} = [\text{1}]/[\text{2}]$, determined spectrophotometrically (640 nm) in dichloromethane. ^c Equilibrium constant of cross reaction $\text{1}^+ + \text{2} \rightleftharpoons \text{2}^+ + \text{1}$ calculated from $K_{\text{cr}} = \exp[(F/RT)(E_{\text{cis}}^\circ - E_{\text{trans}}^\circ)]$. ^d $K_{\text{III}} = [\text{2}^+]/[\text{1}^+]$, estimated from K_{cr} and K_{II} values using $K_{\text{cr}} = K_{\text{II}}K_{\text{III}}$.

† Satisfactory elemental analyses were obtained. Complex **1** is diamagnetic. Complex **2**⁺ has $\mu_{\text{eff}} = 1.87$ μ_{B} at 298 K; EPR g values are $g_1 = 2.751$, $g_2 = 2.552$, $g_3 = 1.447$ in dichloromethane–toluene frozen glass (77 K).

knowledge no thioxanthate of osmium has been reported previously.



Electrochemical and spectral studies have revealed that **1** is stereoretentively electrooxidised to **1**⁺, which then readily

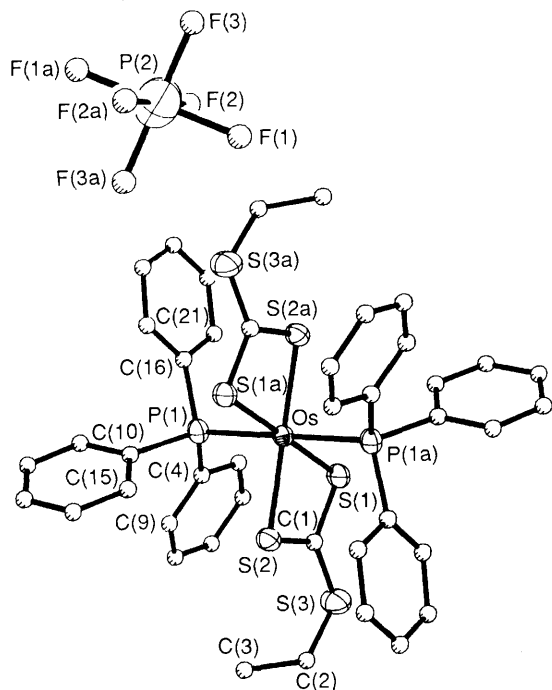
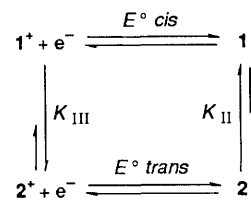


Fig. 1 Perspective view and labelling scheme for *trans*-[Os(EtSCS₂)₂(PPh₃)₂]PF₆²⁺PF₆⁻. Pertinent distances (Å) and angles (°): Os–P(1), 2.425(1); Os–S(1), 2.374(1); Os–S(2), 2.376(1); C(1)–S(1), 1.689(3); C(1)–S(2), 1.696(5); C(1)–S(3), 1.720(4); P(1)–Os–S(1), 93.3(1); P(1)–Os–S(2), 86.2(1); S(1)–Os–S(2), 72.1(1).

undergoes first-order isomerisation (*t*_{1/2} 0.20 s at 303 K) to give **2**⁺; on the other hand **2**⁺ is electroreduced to give **2** which spontaneously rearranges to **1** relatively slowly (*t*_{1/2} 7.4 h at 303 K). Complex **1**⁺ has eluded isolation owing to its short *t*_{1/2}. Equilibria interlinking the OsS₄P₂ species are shown in Scheme 1 and the relevant thermodynamic parameters are collected in Table 1. Thus, Os^{III} and Os^{II} have strong preferences for the *trans*- and *cis*-S₄P₂ configurations respectively. When forced into a 'wrong' (as in **1**⁺ and **2**) geometry by rapid redox isomerisation takes place.

The structural results provide insight into the origin of isomer discrimination by metal oxidation states. All three molecules have crystallographically imposed symmetry; **2** and **2**⁺ are centrosymmetric while **1** has C₂ symmetry and in all three cases the asymmetric unit is the Os(EtSCS₂)(PPh₃) fragment. Comparison of bond parameters is therefore meaningful. Between **2**⁺ and **2** the Os–P distance decreases by ≈ 0.07 Å, from 2.425(1) to 2.357(3) Å. Metal reduction is expected to cause an increase in metal–ligand bond length when the ligand is innocent. This occurs with the Os–S bond, the mean length being 2.375(1) Å in **2**⁺ and 2.406(4) Å in **2**. Thus, the thioxanthate ligand is more or less innocent in the present complexes. The large contraction of the Os–P bond upon metal reduction is attributed to a dramatic strengthening of 5d_π–3d_π back-bonding in the OsP₂ fragment in going from Os^{III} to Os^{II}. The back-bonding order Os^{II} ≫ Os^{III} is not unexpected⁵ but the present work provides a direct structural demonstration.

We now consider the *cis*-isomer **1**. Its Os–P distance is shorter than that in **2** by ≈ 0.05 Å. In octahedral complexes



Scheme 1

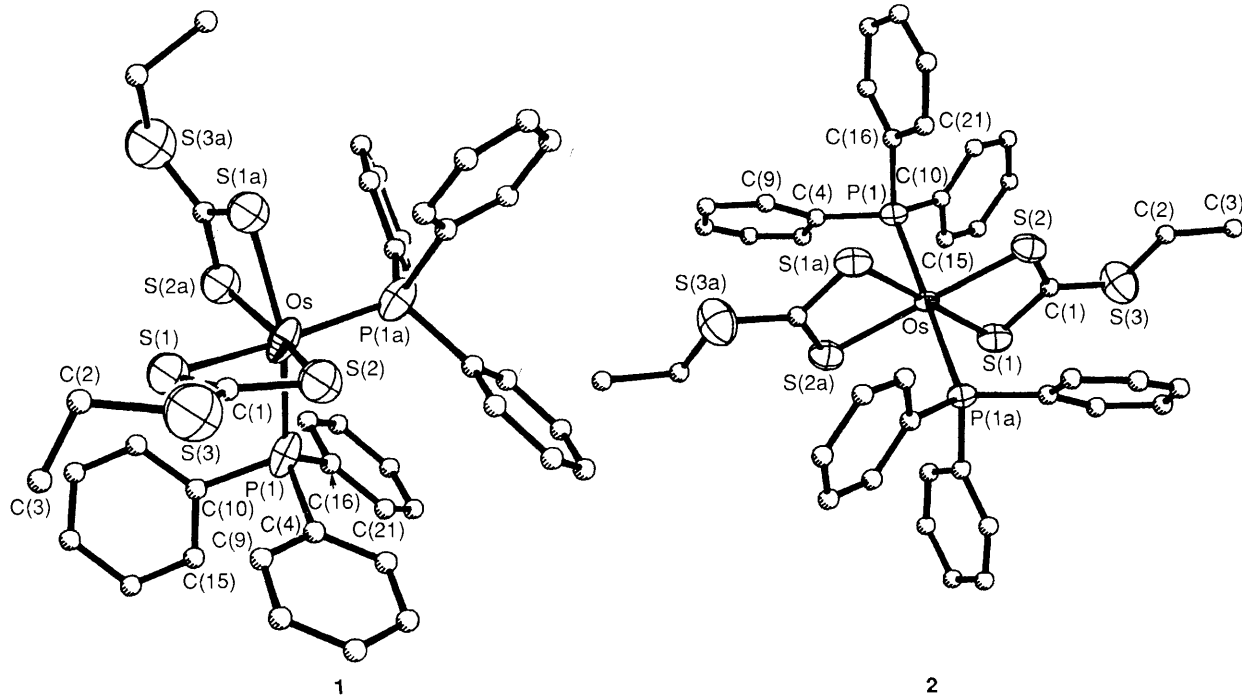


Fig. 2 Perspective view and labelling scheme for *cis*-**1** and *trans*-**2** Os(EtSCS₂)₂(PPh₃)₂. Pertinent distances (Å) and angles (°): for **1**, Os–P(1), 2.310(3); Os–S(1), 2.452(3); Os–S(2), 2.385(3); C(1)–S(1), 1.700(12); C(1)–S(2), 1.658(12); C(1)–S(3), 1.734(11); P(1)–Os–S(1), 90.0(1); P(1)–Os–S(2), 96.0(1); P(1)–Os–P(1A), 100.1(1); S(1)–Os–S(2), 70.7(1); S(1)–Os–S(1A), 83.0(1); S(1)–Os–S(2A), 94.9(1); S(1)–Os–P(1A), 164.2(1); S(2)–Os–S(2A), 161.2(1); for **2**, Os–P(1), 2.357(3); Os–S(1), 2.405(3); Os–S(2), 2.407(4); C(1)–S(1), 1.696(17); C(1)–S(2), 1.680(14); C(1)–S(3), 1.742(12); P(1)–Os–S(1), 94.6(1); P(1)–Os–S(2), 86.6(1); S(1)–Os–S(2), 71.1(2).

back-bonding is expected to be stronger in the *cis*- than in the *trans*-isomer since three and two metal d_{π} orbitals are available for π -acceptance in the two isomers respectively. Owing to the *trans*-influence of the phosphine the two Os–S distances in **1** are unequal: 2.452(3) and 2.385(3) Å. The mean value, however, lies within 0.01 Å of that in **2**. The unfavourable *cis*-PPh₃–PPh₃ interaction⁶ in **1** is structurally reflected in the expected manner:^{6c} an obtuse P(1)–Os–P(1A) angle, 100.1(1)°, and a staggered (C^α)₃P(1)·P(1A)(C^α)₃ conformation. However, the Os^{II} back-bonding factor (strong and *cis* > *trans*) more than offsets the steric disadvantage making the *cis*-geometry more stable. The interplay of the two opposing factors is reflected in the sizable equilibrium concentration of **2** ($K_{II} \approx 10$).

The back-bonding hierarchy *cis* > *trans* is not however of much consequence for Os^{III} since the back-bonding itself is weak. In this situation, PPh₃–PPh₃ steric interaction⁶ becomes strongly controlling. This explains the superior stability of *trans*-**2**⁺ compared to *cis*-**1**⁺: $K_{III} \approx 10^4$. In O_h symmetry Os^{III} would be subject to mild (t_2^5) Jahn–Teller distortion but this effect is unlikely to be significant in the context of isomerisation of the Os^{III} complexes which already have only rhombic symmetry owing to ligand constraints.

In summary the differentiation of geometrically isomeric environments by Os^{II} and Os^{III} in the present group of complexes is based on two primary principles: maximisation of back-bonding where it matters most (Os^{II}: *cis*) and minimisation of steric crowding where back-bonding is weak (Os^{III}: *trans*).

Crystallography was done at the National Single Crystal Diffractometer Facility, Department of Inorganic Chemistry, Indian Association for the Cultivation of Science. Financial support received from the Department of Science and

Technology, New Delhi and the Council of Scientific and Industrial Research, New Delhi, India, is acknowledged.

Received, 1st May 1990; Com. 0101933J

References

- 1 P. Basu, S. Pal and A. Chakravorty, *J. Chem. Soc., Chem. Commun.*, 1989, 977; P. Basu, S. Bhanja Choudhury, S. Pal and A. Chakravorty, *Inorg. Chem.*, 1989, **28**, 2680; D. Ray and A. Chakravorty, *Inorg. Chem.*, 1988, **27**, 3292; N. Bag, G. K. Lahiri and A. Chakravorty, *J. Chem. Soc., Dalton Trans.*, 1990, 1557.
- 2 A. M. Bond, B. S. Grabaric and Z. Grabaric, *Inorg. Chem.*, 1978, **17**, 1013; A. M. Bond, S. W. Carr and R. Colton, *Inorg. Chem.*, 1984, **23**, 2343; A. M. Bond, T. W. Hambley, D. R. Mann and M. R. Snow, *Inorg. Chem.*, 1987, **26**, 2257, and references cited therein.
- 3 R. D. Rieke, H. Kojima and K. Öfele, *J. Am. Chem. Soc.*, 1976, **98**, 6735; C. M. Elson, *Inorg. Chem.*, 1976, **15**, 469; A. Vallat, M. Person, L. Roullier and E. Laviron, *Inorg. Chem.*, 1987, **26**, 332; M. M. Bernardo, P. V. Robandt, R. R. Schroeder and D. B. Rorabacher, *J. Am. Chem. Soc.*, 1989, **111**, 1224.
- 4 B. E. Bursten, *J. Am. Chem. Soc.*, 1982, **104**, 1299; D. M. P. Mingos, *J. Organomet. Chem.*, 1979, **179**, C29.
- 5 H. Taube, *Pure Appl. Chem.*, 1979, **51**, 901; M. Sekine, W. D. Harman and H. Taube, *Inorg. Chem.*, 1988, **27**, 3604.
- 6 (a) C. A. Tolman, *Chem. Rev.*, 1977, **77**, 313; (b) H. C. Clark and M. J. Hampden-Smith, *Coord. Chem. Rev.*, 1987, **79**, 229; (c) J. Powell, *J. Chem. Soc., Chem. Commun.*, 1989, 200.
- 7 A. C. T. North, D. C. Philips and F. S. Mathews, *Acta Crystallogr., Sect. A*, 1968, **24**, 351.
- 8 G. M. Sheldrick, SHELXTL-Plus 88, Structure Determination Software Program, Nicolet Instrument Corp.: 5225–2 Verona Road, Madison, WI 53711, 1988. Computations were carried out on a MicroVAX II computer.